Article Chinese Science Bulletin

Geochemistry April 2013 Vol.58 No.11: 1299–1309
doi: 10.1007/s11434-012-5534-z

Correlation of burial organic carbon and paleoproductivity in the Mesoproterozoic Hongshuizhuang Formation, northern North China

LUO QingYong[1], ZHONG NingNing[1*], ZHU Lei[1], WANG YanNian[1,2], QIN Jing[1,3], QI Lin[1,4], ZHANG Yi[1] & MA Yong[1]

[1] *State Key Laboratory of Petroleum Resources & Prospecting, China University of Petroleum, Beijing 102249, China;*
[2] *Petrochina Coalbed Methane Company Limited, Beijing 100028, China;*
[3] *National Research Center for Geoanalysis, Beijing 100037, China;*
[4] *Chongqing Institute of Geology & Mineral Resources, Chongqing 400042, China*

Received June 1, 2012; accepted October 10, 2012; published online November 30, 2012

In general, total organic carbon (TOC) is directly used as a proxy for paleoproductivity, however, it is not only affected by paleoproductivity, but also controlled by redox conditions and terrigenous detrital matter influx. Major and trace elements were analysed with the purpose of investigating the redox potential and paleoproductivity during deposition of the Hongshuizhuang Formation. In the present study, C-S relationship, V/Cr ratio and Mo concentration indicate that the dolomites were deposited in oxic environments, however, most of the black shales were accumulated in euxinic environments. P/Ti values in the Hongshuizhuang samples can be compared with those in the Japanese Ubara Permian-Triassic section which were regarded to be deposited under a moderate to high paleoproductivity. Ba/Al values are slightly lower than that of the laminated sediments from the continental margins of Central California (CCAL) which were thought to be accumulated under a high paleoproductivity. These results indicate that the paleoproductivity was moderate to high during deposition of the Hongshuizhuang Formation. Burial organic carbon shows positive correlations with V/Cr and Mo, but shows only weakly or no correlation with P/Ti and Ba/Al, respectively, suggesting that although the paleoproductivity was moderate to high during deposition of the Hongshuizhuang Formation, its organic-rich sediments were predominantly controlled by redox conditions and had no direct relationship with paleoproductivity.

burial organic carbon, paleoproductivity, P/Ti, Ba/Al, redox conditions, Hongshuizhuang Formation, Mesoproterozoic

Citation: Luo Q Y, Zhong N N, Zhu L, et al. Correlation of burial organic carbon and paleoproductivity in the Mesoproterozoic Hongshuizhuang Formation, northern North China. Chin Sci Bull, 2013, 58: 1299–1309, doi: 10.1007/s11434-012-5534-z

The definition of paleoproductivity is the velocity of energy fixed by marine organisms during the process of energy cycles, i.e. the amount of organic matter produced in per unit area and per unit time [1]. Paleoproductivity provides source material for the formation of sedimentary organic matter. Usually, total organic carbon (TOC) has been used as a direct paleoproductivity indicator. High TOC is regarded to be related with a high paleoproductivity, while low TOC is thought to be a direct result of a low paleoproductivity. However, TOC is a biogeochemical product during the carbon cycle and is the sedimentary and preserved organic carbon in the sediments after the primary producers experienced the processes of generation, death, decomposition, mineralization and so on [2]. Therefore, the present-day meseared TOC in sediments represents the burial organic matter, i.e. burial organic carbon. Thus it can be seen that TOC in the marine sediments is not only controlled by paleoproductivity, but also by decomposition velocity, preservation and terrigenous detrital matter influx [3–5]. So the dicussion of the relationship between burial organic carbon and paleoproductivity will be helpful to evaluate the paleoproductivity. Trace elements that reflect the habitat, nutriture and sedimentary environments, such as biogenic barium, phosphrous, Al/Ti, authigenic U and so on,

*Corresponding author (email: nnzhongxp@cup.edu.cn)

are widely used to assess paleoproductivity [6–19]. Dean et al. [20] proposed Ba/Al to evaluate the paleoproductivity of the laminated sediments in the central California (CCAL) margins during the last interstadial (OIS-3, ca. 60–24 ka) and found that Ba/Al as a paleoproductivity indicator and TOC/Al as a redox proxy showed an apparent positive correlation. Algeo et al. [21] used excess Ba (Ba_{ex}) and P/Ti as paleoproductivity proxys in two Permian/Triassic boundary sections (Ubara and Gujo-Hachiman) in central Japan. The average TOC in the two sections is 0.13% and 0.19%, respectively, however, they were deposited in a moderate to high productivity location. It is thus clear that the relationship between paleoproductivity and TOC is not the same under different geological settings so that it is important to discuss the correlation between them.

The sediments of the Mesoproterozoic Hongshuizhuang Formation are predominantly a succession composing of black shales and dolomites in the northern north China. The balck shales are rich in organic matter and are regarded as one of the oldest organic-rich sediments and hydrocarbon rocks in China [22]. During the Mesoproterozoic, there were no higher plants. The biological source of organic matter were mainly plankton. The biodiversity is single and the burial organic carbon in the sediments is mainly derived from the marine primary productivity. Therefore, the Hongshuizhuang Formation samples are good materials for discussing the correlation between burial organic carbon and marine paleoproductivity. Researching on the paleoproductivity during deposition of the Hongshuizhuang Formation is of great importance to the Mesoproterozoic carbon cycle among atmosphere, hydrosphere, biosphere and lithosphere.

1 Geological setting

According to the tectonic subdivision, the Yanshan basin can be divided into five sags and two uplifts which include Liaoxi sag, Shanhaiguan uplift, Jibei sag, Jidong sag, Jingxi sag, Mihuai uplift and Xuanlong sag from east to west (Figure 1). Meso-Neoproterozoic in the Yanshan basin belongs to the aulacogen sediment [23,24]. The structure history during Meso-Neoproterozoic in the Yanshan basin was mainly controlled by the emergence and evolution of the Yanshan aulacogen. Evolution of the Yanshan aulacogen can be divided into three stages: early emergence (1800–1600 Ma), middle development (1600–1400 Ma) and late extinction (1400–1300 Ma) [22]. The Meso-Neoproterozoic in this region can be differentiated into 3 systems and 12 formations from bottom to top (Figure 2). Recent chronological researches reveal that ages of the Xiamaling Formation and Tieling Formation overlying the Hongshuizhuang Formation were 1327–1368 Ma [25–28,[1)]] and 1437±21 Ma

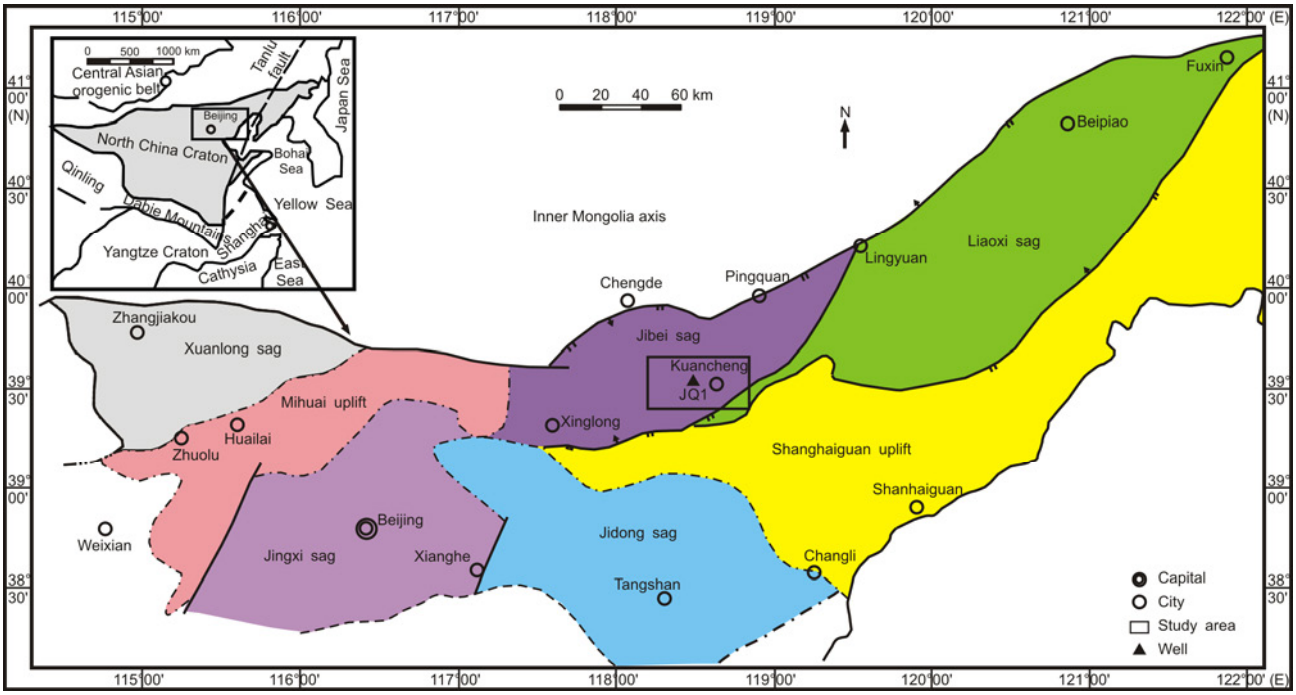

Figure 1 Tectonic subdivisions of the northern North China.

1) Zhong N N, Zhang Z H, Huang Z L, et al. Histories of hydrocarbon generation and charging of Mesoproterozoic sediments in north China. A report for the project of Sinopec Marine Prospecting Program (YPH-08-028). 2009 (unpublished).

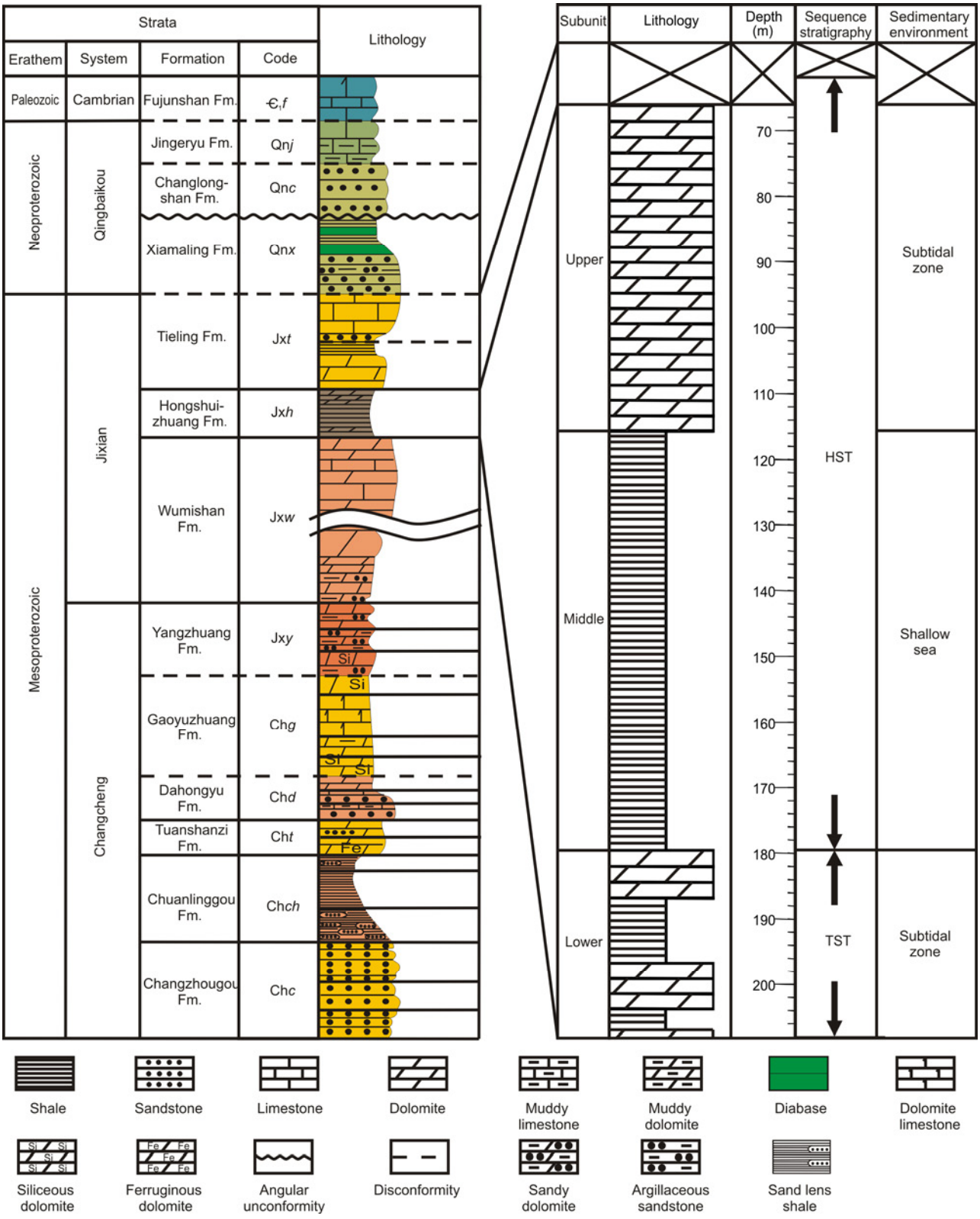

Figure 2 Stratigraphic column of the Meso-Neoproterozoic section intersected by well JQ1. Fm, Formation; HST, Highstand System Tract; TST, Transgressive System Tract.

[28], respectively. Therefore, the age of the Hongshuizhuang Formaiton was older than 1400 Ma which is in correspondence with the early period of the Yanshan aulacogen late extinction stage.

The well JQ1 which is located in the Jibei sag of the Yanshan basin, nothern north China (Figure 1), was drilled

to the full section of the Hongshuizhuang Formation. The thickness of the Hongshuizhuang Formation is about 140 m in the well. The Foramtion can be divided into three lithological subunits from bottom to top. The lower subunit consists of thin black siliceous shales and argillaceous dolomites with rhythmic bedding that reflects a subtidal sedimentary environment, and comprises a 'third-sequence' transgressive system tract (TST). The middle subunit consists of black shales with disseminated pyrites and small amounts of glauconites, consistent with sedimentation in a shallow sea environment representing the period of deepest water during deposition of the Hongshuizhuang Formation [29–32]. The upper subunit includes silty dolomites with micritic dolomite towards the top, indicating water shoaling to a subtidal environment (Figure 2). The middle-to-upper subunits of the Hongshuizhuang Formation together with the lower part of the Tieling Formation constitute a 'third-sequence' highstand system tract (HST) (Figure 2).

2 Sampling and experimental

A total of 47 samples of depths between 65 and 210 m (Table 1) were collected from well JQ1. The samples were ground in an agate mortar and pestle to −200 mesh size. For TOC analyses, a 0.10 g sample was treated in a sterilized crucible with 12.5% HCl to remove carbonates, then washed with distilled water at intervals of about half an hour for three days. The samples were eventually oven-dried and residual organic carbon was measured using a Leco CS230 analyzer.

Al_2O_3 concentrations were determined at the China University of Mining and Technology (Beijing) by X-ray fluorescence (XRF), using an ARL ADVANT'X. Al content was caclulated according to the molecular weight of Al_2O_3. The pyrite sulfur (S_p) extraction procedure is based on the Chromium reduction method [33–35]. 0.5 g shale or 5.00 g dolomite reacted with 20 mL HCl (1 mol/L). The 10 mL $CrCl_2$ (1 mol/L) was added to the residual solution and heated on an electrical heating jacket, which would make S_p transform into H_2S. H_2S was converted into Ag_2S by reacting with $AgNO_3$ solution. The latter two steps were under the N_2 atmosphere. Weigh Ag_2S after drying, then S_p can be calculated based on the molecular weight of Ag_2S.

The samples were prepared for trace and major elements' analyses using about 25 mg of powdered and homogenized sample loaded in polytetrafluoroethylene (PTFE) vessels and heated to 190°C for 72 h in PTFE autoclaves with 1 mL HF (40%) and 1 mL HNO_3 (65%). Acids were removed by evaporation at 200°C on hot plates, and the wet residues were twice redissolved and re-evaporated using 0.5 mL HNO_3 (65%). After the final HNO_3 treatment, wet residues were again heated to 130°C for 12 h in PTFE autoclaves with 5 mL HNO_3 (32.5%). The wet residues were diluted to 30 mL with 2% HNO_3. For analysis, the acid digestions were spiked with Rh and Re as internal standards. The Chinese standard matters GB7107 (shale) and GB7114 (dolomite) were used to check the accuracy of the analyses. The detection limit of V, Cr and Mo is 0.01 ppm, 0.1 ppm for Ba, 1 ppm for P and Ti. Measurements were carried out using a Perkin Elmer Elan DRC-e ICP-MS in the State Key Laboratory of Petroleum Resource and Prospecting, China University of Petroleum, Beijing.

3 Results and discussion

Table 1 shows the measurement results and inorganic geochemical parameters of the Hongshuizhuang Formation for JQ1 samples.

3.1 The relationship between the burial organic carbon and sulfur in the pyrite

As shown in Table 1, TOC of the dolomites ranges from 0.08% to 0.65%, averaging 0.30%. The dolomites contain between 0.01% and 1.16% S_p, with a mean of 0.25%. TOC falls between 0.41% and 8.00% in the black shales, with an average of 3.56%, however, S_p spans from 0.31% to 2.87%, with a mean of 1.11%. Therefore, the TOC and S_p in the black shales are apparently higher than those of the dolomites.

C-S relationship was widely used to evaluate the redox conditions during deposition of the sediments [4,36–39]. In the normal marine (oxic) environments, the oxic-anoxic boundary is under the sediment-water interface. So the sulfates were reduced to form pyrite by organic matter below the sediment-water interface. Iron participating in the sulfate reaction was derived from the detrital matter in the sediment, so the Fe supply was enough in the system. So the pyrite formation was mainly controlled by the burial organic matter under this circumstance. Therefore, the ratio of the organic matter participating in sulfate reduction reaction and the sulfur in the pyrite was certain. Simillarly, the ratio of the organic matter that participated in sulfate reduction reaction and the originally buried organic matter was certain too. The conclusion which can be inferred from these results is that the remaining burial organic matter (TOC) and S_p show a positive correlation, and show a zero intercept because if there were no organic matter in the system, the sulfate reduction reaction would not happen and thus no pyrite was formed [36–39]. On the other hand, under anoxic or euxinic environments, the oxic-anoxic boundary is in the water column. In this case, the H_2S is enough in the water column, so the pyrite formation which was happened in the water column is primarily influenced by availability iron. Therefore, A plot of TOC and S_p shows no direct correlation between the two variables, and shows a nonzero sulfur intercept because even if there is no organic matter in the sediment, there are enough free H_2S for pyrite formation in

Table 1 Geochemical data of the Hongshuizhuang Formation samples from well JQ1

Sample	Lithology	Depth (m)	TOC (%)	S_p (%)	V (ppm)	Cr (ppm)	V/Cr	Mo (ppm)	Al (%)	Ti (ppm)	P (ppm)	P/Ti	Ba (ppm)	Ba/Al[a)]
H-47	dolomite	66.18	0.11	0.02	2.86	6.16	0.46	0.48	0.35	139	265	1.91	21.3	60.34
H-46	dolomite	66.68	0.64	0.14	14.03	13.70	1.02	0.04	2.27	961	194	0.20	98.7	43.48
H-45	dolomite	69.18	0.08	0.07	2.35	6.43	0.37	–[b)]	0.66	362	185	0.51	111.0	169.21
H-44	dolomite	72.94	0.15	0.06	24.60	21.10	1.17	–	3.14	1490	261	0.18	181.0	57.64
H-43	dolomite	79.19	0.24	0.01	8.87	11.80	0.75	0.14	1.34	634	282	0.44	115.0	85.82
H-42	dolomite	81.33	0.38	0.14	48.90	36.65	1.33	0.43	5.24	2395	329	0.14	318.5	60.78
H-41	dolomite	91.71	0.23	0.15	47.40	37.10	1.28	–	5.33	2660	513	0.19	343.0	64.35
H-40	dolomite	96.58	0.16	0.08	60.00	44.50	1.35	0.03	5.39	2980	444	0.15	384.0	71.24
H-39	dolomite	100.83	0.29	0.03	41.40	40.00	1.04	–	5.48	2450	393	0.16	795.0	145.07
H-38	dolomite	106.74	0.22	0.16	52.40	37.50	1.40	–	5.49	2490	431	0.17	324.0	59.02
H-37	dolomite	108.99	0.31	0.27	64.30	49.10	1.31	–	6.13	3025	586	0.19	424.0	69.17
H-36	dolomite	111.56	0.28	0.16	50.70	39.50	1.28	–	5.53	2630	453	0.17	357.0	64.56
H-35	shale	116.85	4.67	1.92	592.00	83.50	7.09	55.90	6.50	3150	1340	0.43	493.0	75.85
H-34	shale	118.96	4.67	1.31	548.00	64.00	8.56	43.10	5.92	2960	1360	0.46	498.0	84.12
H-33	shale	120.63	4.50	1.44	565.00	57.00	9.91	34.70	6.33	3020	1380	0.46	508.0	80.25
H-32	shale	123.86	3.92	1.25	598.00	77.40	7.73	44.20	6.61	3220	1620	0.50	505.0	76.40
H-31	shale	126.61	4.10	1.25	477.00	77.10	6.19	58.30	6.74	3410	1190	0.35	545.0	80.86
H-30	shale	129.43	3.30	0.78	304.00	53.70	5.66	32.40	6.45	2880	1080	0.38	499.0	77.36
H-29	shale	133.01	3.85	1.27	484.00	64.00	7.56	58.50	6.00	3240	1560	0.48	560.0	93.33
H-28	shale	136.33	4.74	2.10	487.00	58.90	8.27	62.90	5.52	2630	1860	0.71	454.0	82.25
H-27	shale	139.83	5.46	0.64	296.50	48.50	6.11	43.95	4.69	2380	1650	0.69	413.5	88.17
H-26	shale	141.56	5.72	1.94	345.00	50.60	6.82	54.80	4.75	2310	2010	0.87	420.0	88.42
H-25	shale	145.56	5.30	1.63	365.00	42.00	8.69	50.30	4.67	2180	1930	0.89	410.0	87.79
H-24	shale	148.16	1.33	2.87	140.00	21.60	6.48	5.29	2.82	1270	491	0.39	188.0	66.67
H-23	shale	151.56	5.18	1.27	350.00	44.30	7.90	27.30	5.05	2410	1990	0.83	433.0	85.74
H-22	shale	154.69	1.31	0.93	44.45	35.70	1.25	0.64	5.14	2180	871	0.40	430.5	83.75
H-21	shale	156.84	1.18	0.84	57.30	40.40	1.42	1.12	6.00	2710	1010	0.37	541.0	90.17
H-20	shale	160.43	0.70	0.38	56.40	50.10	1.13	0.69	7.02	3070	1040	0.34	499.0	71.08
H-19	shale	163.02	2.89	0.99	80.20	64.20	1.25	3.37	6.17	2420	800	0.33	736.0	119.29
H-18	shale	166.11	3.73	0.73	131.00	52.70	2.49	6.93	5.79	2600	1580	0.61	485.0	83.77
H-17	shale	169.3	4.07	1.15	334.50	70.30	4.76	16.35	5.92	2885	1845	0.64	479.5	81.00
H-16	shale	172.38	4.41	0.89	294.00	50.40	5.83	13.10	5.27	2390	1550	0.65	508.0	96.39
H-15	shale	175.57	4.95	1.40	290.00	45.80	6.33	27.90	4.67	2160	1520	0.70	643.0	137.69
H-14	shale	177.05	3.51	0.31	201.00	41.70	4.82	5.58	4.50	1980	793	0.40	390.0	86.67
H-13	shale	179.05	0.82	0.81	64.40	53.30	1.21	–	6.35	3350	2190	0.65	412.0	64.88
H-12	dolomite	179.72	0.46	0.24	31.00	61.00	0.51	0.58	3.67	1820	1390	0.76	340.0	92.64
H-11	dolomite	180.69	0.35	0.73	15.85	15.75	1.01	0.24	1.89	865	684	0.79	130.0	68.78
H-10	dolomite	190.78	0.21	0.64	6.87	15.50	0.44	0.39	1.25	450	477	1.06	68.6	54.88
H-9	shale	194.17	1.00	1.89	253.00	83.80	3.02	5.14	7.61	3930	2710	0.69	576.0	75.69
H-8	shale	195.09	0.93	0.47	22.70	19.90	1.14	0.89	2.34	860	719	0.84	203.0	86.75
H-7	shale	195.76	5.67	0.66	212.00	48.30	4.39	15.50	4.34	2050	2070	1.01	360.0	82.95
H-6	shale	196.73	0.41	0.80	42.00	31.90	1.32	1.22	4.49	1540	1200	0.78	222.0	49.44
H-5	dolomite	200.9	0.65	1.17	13.15	13.70	0.96	0.62	1.58	553	654	1.18	79.5	50.32
H-4	shale	205.01	4.67	0.62	110.00	45.80	2.40	6.76	4.25	1800	1620	0.90	416.0	97.88
H-3	shale	205.31	4.13	0.64	62.20	42.60	1.46	2.88	4.09	1860	1930	1.04	364.0	89.00
H-2	shale	206.92	1.25	0.66	29.10	38.60	0.75	1.01	3.73	1550	1150	0.74	286.0	76.68
H-1	shale	207.58	8.00	0.84	116.00	90.20	1.29	14.00	7.21	3590	2670	0.74	285.0	39.53

a) The unit of Ba/Al is ppm/%; b) "–" represents that the concentration of elements is lower than 0.01 ppm.

the water column or sediment [36–39].

As shown in Figure 3, TOC and S_p show a positive correlation (r=0.71) in the dolomites and part of black shales (TOC<2%), and the intercept is close to 0, which indicate these sediments were deposited in oxic environments. TOC and S_p show no direct correlation (r=0.14) in other black shales (TOC>2%), and the intercept on the S_p axis is 0.88%, which suggest that they might be deposited under anoxic or euxinic environments.

3.2 The redox conditions during the deposition and burial of organic carbon

The dolomites of the Hongshuizhuang formation contain between 0.37 and 1.40 V/Cr, with a mean of 0.98. V/Cr spans from 1.13 to 9.91 in the black shales, averaging 4.91 and maxing at 120 m (Figure 4 and Table 1). V/Cr remains nearly constant from the lower subunit to the lower part of the middle subunit (only showing variation at 195.76–194.17 m), then increases suddenly and reaches the maximum 6.33 at around 175 m, subsequently decreases slowly and continues at about 1 at 163–155 m, then increases and keeps on between 6 and 10, eventually endures at 1 in the dolomites of the upper subunit.

In oxygenated envrionments, V^{5+} is found in the form of vanadate [40], however, under anoxic or euxinic environments, V^{5+} is reduced to form $VO(OH)_2$ or organometallic ligands or vanadium porphyrin or V_2O_3 or $V(OH)_3$ which then can be enriched in the sediment [41–46]. Under oxic seawater, Cr is present mainly as Cr^{4+} in the chromate anion [47]; however, in anoxic circumstances, Cr^{4+} is reduced to Cr^{3+} which is mainly enriched in the sediment as Cr_2O_3 or $Cr(OH)_3$ or complexation with humic/fulvic acids or adsorption on Fe- and Mn-oxyhydroxides [48,49]. Under euxinic environment, Cr^{3+} adsorption by authigenic Fe-sulfides is very limited [50,51]. In addition, the insoluble chromium sulfide is not present so far [51].

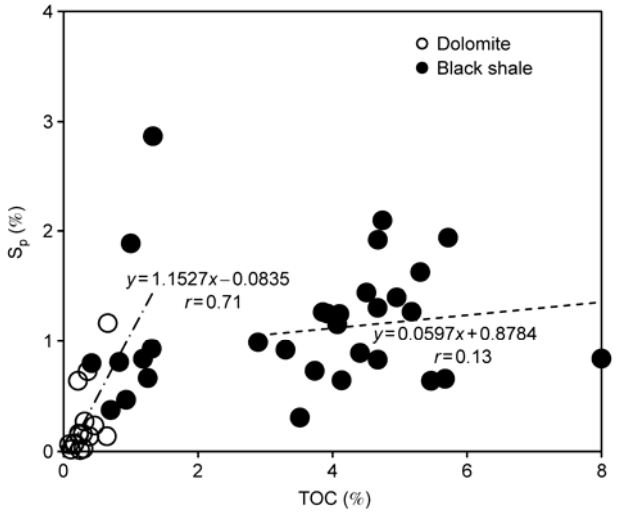

Figure 3 Crossplot of TOC and pyrite S of the Hongshuizhuang Formation samples. The chain line represents the trend line of TOC and pyrite S for dolomites and black shales (TOC<2%); the dotted line is for black shales (TOC>2%).

Based on the behavior of V and Cr as stated above, Jones et al. (1994) [52] proposed V/Cr ratio to evaluate redox conditions. A V/Cr ratio <2 suggests oxic conditions, 2–4.25 implies suboxic conditions, and >4.25 represents anoxic to euxinic conditions. V/Cr values are smaller than 2 in the dolomites, suggesting that the dolomites were deposited in oxic environments. Most of the black shales contain V/Cr larger than 4.25, especially the shales from the upper (116.85–151.56 m) and lower (166.11–177.05 m) parts of the middle subunit, indicating most of the black shales were deposited in anoxic or euxinic environments. More specifically, the black shales in the middle (154.69–163.02 m) and bottom-most (179.05 m) parts of the middle subunit contain low V/Cr, smaller than 2, suggesting they were derived from oxic environments. V/Cr values range between 0.75 and 4.39 in the black shales from the lower subunit, suggesting the redox environments were turbulent (oxic to euxinic) (Figure 4 and Table 1).

The Mo contents with depth are in a similar trend with V/Cr (Figure 4). As shown in Table 1, Mo contents in the dolomites are either lower than the detection limit or in the range of 0.03 to 0.62 ppm. In oxic seawater, Mo is present as stable MoO_4^{2-} [53]. The residual MoO_4^{2-} may be transferred to sediment-water interfaces by adsorption onto Mn-oxyhydroxides and humic substances [54–56]. Below the oxic-anoxic interface, Mo was released to pore water because of the reductive dissolution of Mn-oxyhydroxide particles [55], which can explain the enrichment of Mo at or near oxic-anoxic interface, but can not explain its enrichment in the sediment [46]. Helz et al. [56] proposed that one S^{2-} can replace one O^{2-} in MoO_4^{2-} in the presence of H_2S to create thiomolybdates ($MoO_xS_{4-x}^{2-}$, x=0 to 3), which makes Mo become a particle-reactive species and then can be enriched in the sediments [54,57]. The Mo contents in the dolomites are even lower than those of terrigenous detrital matter (1 ppm) [20] and plankton (2 ppm) [58], indicating no enrichment of Mo. Therefore, the dolomites were deposited under oxic environments.

As stated above, Mo is only enriched in euxinic environments, so Mo was regarded as the best diagnosis to distinguish anoxic and euxinic environments [59]. Mo ranges from 5.29 to 62.90 ppm in the black shales from the the upper part (116.85–151.56 m) of the middle subunit and falls between 5.58 and 27.90 ppm in the black shales from the lower part (166.11–177.05 m) of the middle subunit. Although these Mo contents are lower than that of the sediments from balck sea (150 ppm) [60], they are higher than those of the detrital matter (1 ppm) [20] and plankton (2 ppm) [58]. At the same time, Piper (1994) [61] and Crusius et al. [55] suggested that 5–40 ppm Mo implies euxinic environment. So euxinic environments was related with the black shales from the the upper and lower parts of the middle

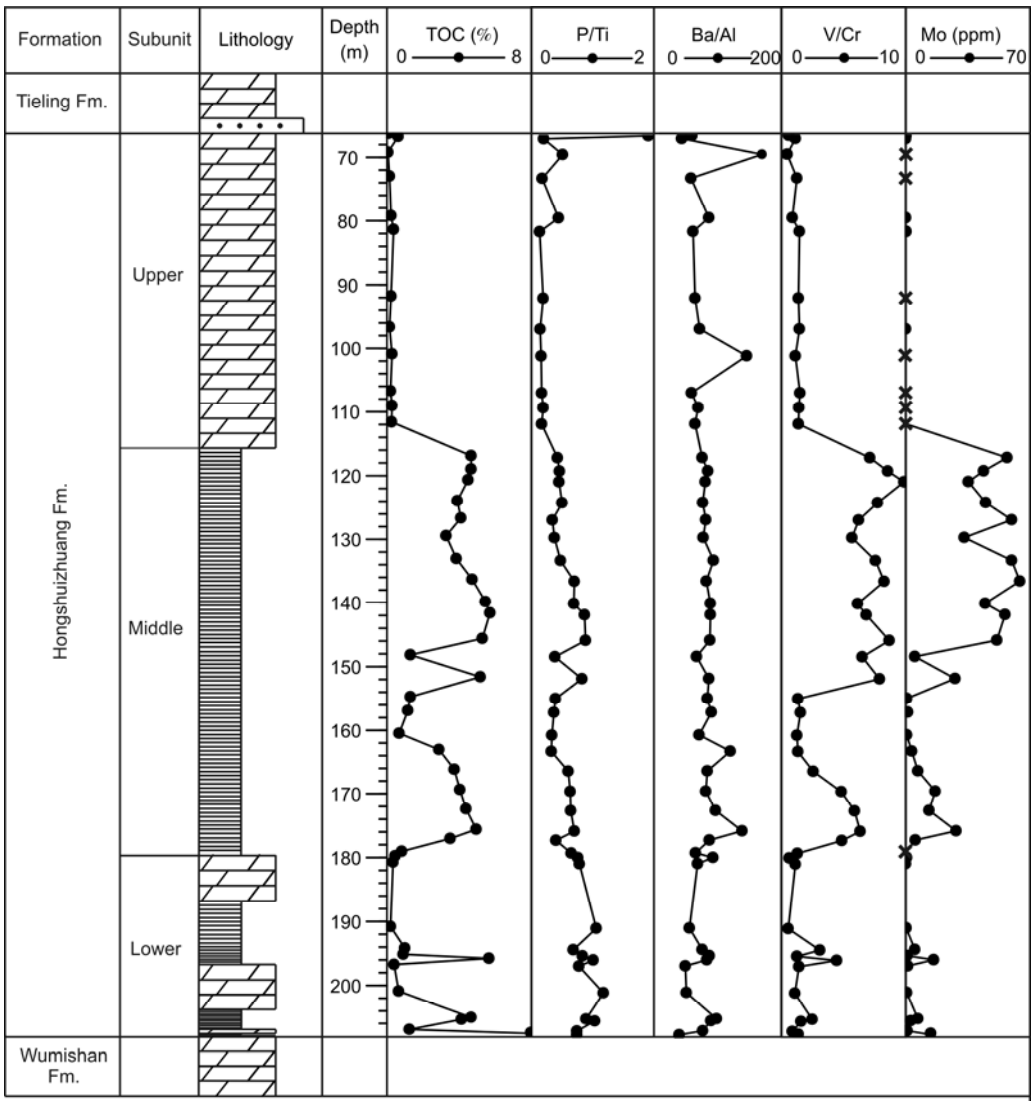

Figure 4 Profiles of TOC, P/Ti, Ba/Al, V/Cr and Mo in the Hongshuizhuang Formation samples from well JQ1. "×" indicates Mo content is lower than the detection limit.

subunit. The black shales of the middle (154.69–163.02 m) and bottom-most (179.05 m) parts of the middle subunit contain low Mo, lower than 2 ppm except one sample, suggestive of oxic environment. Mo concentrations in the black shales of the lower subunit are lower than that of the black shales from the upper part of the middle subunit, and part of them are even lower than 5 ppm, also indicating redox environments are turbulent (Figure 4, Table 1).

3.3 Paleoproductivity during the deposition of the Hongshuizhuang Formation

(1) P/Ti ratio. N and P are the most important nutrient elements for plankton. Plaeoproductivity in marine environments is mainly controlled by the availability of N and P [62]. However, marine photosynthesizers can fix N_2 in the atmonsphere [63], so P was regarded as the ultimate limiting factor in marine environments [53,63,64]. In addition, P is a major constituent of skeletal material and plays a fundamental role in many metabolic processes [46]. For these reasons, sedimentary records of P content was widely used as an indicator for paleoproductivity [3,13,21].

Organic matter and authigenic minerals may have a dilution effect on the absolute P content in terrigeneous detrital matter. In order to mitigate this effect, P/Ti or P/Al is used to evaluate the paleoproductivity rather than the absolute P content [13,21], because Ti or Al generally originates from terrigenous detrital matter [54,57]. In other words, P/Ti or P/Al can represent a nutrient condition of the ancient sea.

In the studied samples, P/Ti is increasing with depth (Figure 4). In the lower subunit, P/Ti ratios range from 0.69 to 1.18, averaging 0.88 (Table 2). The average is similar to that of the black shales in the Ubara section (0.79) which were thought to be a character of a high paleoproductivity

Table 2 Statistics of TOC, P/Ti and Ba/Al for the Hongshuizhuang Formation samples from well JQ1

Subunit	Depth (m)	Sample counts	TOC (%)			P/Ti			Ba/Al		
			Min	Max	Average	Min	Max	Average	Min	Max	Average
Upper	66.18–115.64	12	0.08	0.64	0.26	0.14	1.91	0.37	43.48	169.21	79.22
Middle	115.64–179.42	23	0.70	5.72	3.67	0.33	0.89	0.54	64.88	137.69	86.17
Lower	179.42–208	12	0.21	8.00	2.31	0.69	1.18	0.88	39.53	97.88	72.05

during their deposition [21]. So the lower subunit was deposited under a high paleoproductivity. In the middle subunit, P/Ti ratios fall between 0.33 and 0.89, with a mean of 0.54 (Table 2). This mean is among those of the cherts (0.34) and the black shales in the Ubara section. The cherts in the Ubara section were thought to be deposited under a moderate paleoproductivity [21]. Therefore, the paleoproductivity was moderate to high during depostion of the middle subunit. In the upper subunit, P/Ti ratios range from 0.14 to 1.91, averaging 0.37 (Table 2), similar to that of the cherts (0.34) in the Ubara section [21], indicating a moderate paleoproductivity during their depostion.

(2) Ba/Al ratio.The barite accumulation rate shows a positive correlation with primary productivity in the marine sediments [7–10]. Although it remains controversial whether the non-hydrothermal barite is related with organisms, barite had been usually used as an indicator for paleoproductivity [7–10]. Barite is the main carrier phase of Ba. Dean et al. (1997) [20] suggested Ba/Ti or Ba/Al ratios can be used to qualitatively assess the paleoproductivity. Ti or Al is also used as the denominator in order to eliminate the dilution effect of other components [57]. Both ratios may represent the amount of organisms in the ancient sea.

The lower, middle, and upper subunits contain 39.53–97.88 Ba/Al, averaging 72.05; 64.88–137.69 Ba/Al, with a mean of 86.17; 43.48–169.21 Ba/Al, with an average of 79.22 (Table 2), respectively. Sulfates are reduced after the exhaustion of oxygen, nitrates, Mn/Fe oxides and oxyhydroxides under anoxic environments. Barite dissolution results in Ba^{2+} being mobilized to an SO_4^{2-}-rich zone [58,65,66]. Although the averages of Ba/Al for the three subunits are low, most of the shales were deposited in euxinic environments, so some of Ba in the shales might have been mobilized. Moreover, Ba/Al average ratios for the three subunits are only slightly lower than that (around 100–120) of laminated sediments in CCAL cores which was regarded to be depostited under a high paleoproductivity [20]. These indicate that the Hongshuizhuang Formation was deposited under a moderate-high paleoproductivity, consistent with interpretations based on the P/Ti values.

3.4 Correlation between burial organic carbon and paleoproductivity

Burial organic carbon was simply used as a direct paleoproductivity indicator; however, Burial organic carbon is not only affected by paleoproductivity, but also redox conditions and terrigeneous detrital matter influx. Anoxic environments favor the preservation of organic matter, but oxic environments usually consume the organic matter. The high terrigeneous detrital matter influx dilute the organic matter, however, the low influx is not in favor of the preservation of organic matter. Therefore, burial organic carbon does not represent the content of the original organic matter.

As shown in Table 2, although the average of burial organic carbon in the middle subunit is higher than the lower subunit, the paleoproductivity of the middle subunit is lower than the lower subunit. In addition, in the samples at 180–200 m, the trend of burial organic carbon is opposite to P/Ti or Ba/Al (Figure 4). As shown in Figure 5(a) and (b), burial organic carbon in the black shales with TOC>2% is increasing with the increasing P/Ti, however, burial organic carbon show no apparent variation with the increasing of P/Ti and Ba/Al in the dolomites and the black shales with TOC<2%, especially in the dolomites. This suggests that burail organic carbon as a paleoproductivity proxy may underestimate the paleoproductivity of the dolomites and the black shales with TOC<2%.

In the present study, TOC shows strong positive correlations with the redox proxies V/Cr and Mo (r=0.75 and 0.85, respectively), however, TOC shows weak or no correlations with the paleoproductivity indicators P/Ti and Ba/Al (r= 0.39 and 0.19, respectively) (Figure 5). In addition, as shown in Figure 4, the trend with depth of the TOC contents is similar to those of V/Cr and Mo, but differs from those of P/Ti and Ba/Al. So the sediments were deposited under a moderate to high paleoproductivity regardless of the high or low burial organic carbon. The variation of the burial organic carbon was mainly controlled by redox conditions.

4 Conclusions

(1) Although the burial organic carbon in the marine sediments is an important record of primary productivity, burial organic carbon and paleoproductivity show no direct correlation. The burial organic carbon also may be affected by redox and terrigeneous detrital matter influx.

(2) The nutrient conditions were fine in the sea during the deposition of the Hongshuizhuang Formation. The sediments were associated with a moderate to high paleoproductivity regardless of its high or low burial organic carbon. The

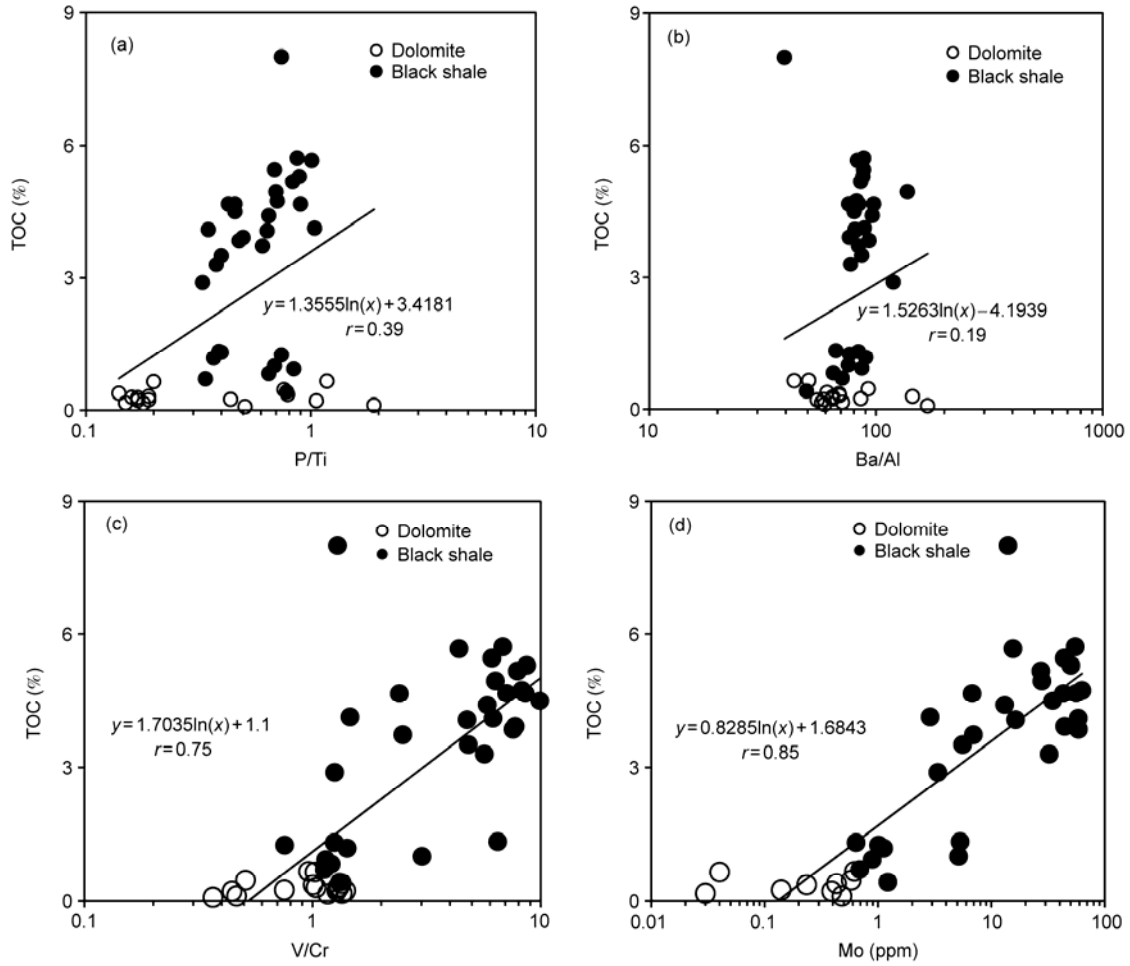

Figure 5 Relationship between (a) P/Ti; (b) Ba/Al; (c) V/Cr; (d) Mo, and TOC in the Hongshuizhuang Formation samples from well JQ1. The solid line is the trend line for the parameters of all Hongshuizhuang Formation samples.

content of the burial organic carbon was primarily controlled by redox environments.

(3) The dolomites of the Hongshuizhuang Formation were deposited in oxic environments as indicated by C-S relationship, V/Cr and Mo, however, most of black shales were related with euxinic environments. This difference in redox conditions determines the content of burial organic carbon.

This work was supported by the National Science and Technology Major Project (*2011ZX05018-002*) *and the National Natural Science Foundation of China* (*40472076*). *The authors would like to thank Associate Professor Wang Chunjiang for providing samples, Zhang Qiangbin, Zhu Wenjuan and Huang Wei for technical support and analytical advice in trace element analysis, and Associate Professor Zhang Tonggang for help in the pyrite sulfur* (S_p) *extraction.*

1 Dong J S, Wan X Q. The preliminary study of paleoproductivity at Neogene period in Zhujiangkou basin (in Chinese). In: Neogene Microfossil and Paleooceanography Study of Zhujiangkou Basin in South China Sea. Wuhan: China University of Geosciences Press, 1996. 129
2 Zhang H F, Fang C L, Gao X Z, et al. Petroleum Geology (in Chinese). Beijing: Petroleum Industry Press, 1999. 1–338
3 Pujol F, Berner Z, Stüben D. Palaeoenvironmental changes at the Frasnian/Famennian boundary in key European sections: Chemostratigraphic constraints. Palaeogeogr Palaeoclimatol Palaeoecol, 2006, 240: 120–145
4 Rimmer S M, Thompsona J A, Goodnighta S A, et al. Multiple controls on the preservation of organic matter in Devonian-Mississippian marine black shales: Geochemical and petrographic evidence. Palaeogeogr Palaeoclimatol Palaeoecol, 2004, 215: 125–154
5 Turgeon S, Brumsack H J. Anoxic vs dysoxic events reflected in sediment geochemistry during the Cenomanian-Turonian Boundary Event (Cretaceous) in the Umbria-Marche Basin of central Italy. Chem Geol, 2006, 234: 321–339
6 Goldberg E D, Arrhenius G O S. Geochemistry of Pacific pelagic sediments. Geochim Cosmochim Acta, 1958, 13: 153–212
7 Dymond J, Suess E, Lyle M. Barium in deep-sea sediment: A geochemical proxy for paleoproductivity. Paleoceanography, 1992, 7: 163–181
8 Dymond J, Collier R. Particulate barium fluxes and their relationships to biological productivity. Deep-Sea Res, 1996, 43: 1283–1308
9 Paytan A, Kastner M, Chavez F P. Glacial to interglacial fluctuations in productivity in the equatorial Pacific as indicated by marine barite. Science, 1996, 274: 1355–1357
10 Paytan A, Griffith E M. Marine barite: Recorder of variations in ocean export productivity. Deep-Sea Res II, 2007, 54: 687–705
11 Ingall E D, Bustin R M, VanCappellan P. Influence of water column anoxia on the burial and preservation of carbon and phosphorus in marine shales. Geochim Cosmochim Acta, 1993, 57: 303–316

12 Filippelli G M, Delaney M L. The oceanic phosphorus cycle and continental weathering during the Neogene. Paleoceanography, 1994, 9: 643–652
13 Latimer J C, Filippelli G M. Eocene to Miocene terrigenous inputs and export production: Geochemical evidence from ODP Leg 177, Site 1090. Palaeogeogr Palaeoclimatol Palaeoecol, 2002, 182: 151–164
14 Murray R W, Leinen M, Isern A R. Biogenic flux of Al to sediment in the central equatorial Pacific Ocean: Evidence for increased productivity during glacial episodes. Paleoceanography, 1993, 8: 651–670
15 Murray R W, Leinen M. Scavenged excess aluminum and its relationship to bulk titanium in biogenic sediment from the central equatorial Pacific Ocean. Geochim Cosmochim Acta, 1996, 60: 3869–3878
16 Kumar N, Anderson R F, Biscaye P E. Remineralization of particulate authigenic trace metals in the Middle Atlantic Bight: Implications for proxies of export production. Geochim Cosmochim Acta, 1996, 60: 3383–3397
17 Wang R J, Li J R. Quaternary high-resolution opal record and its paleoproductivity implication at ODP Site 1143, southern South China Sea (in Chinese). Chin Sci Bull (Chin Ver), 2003, 48: 74–77
18 Li J R, Wang R J, Li B H. Opal accumulation rates and paleo-productivity variation from 12 Ma in the south of South China Sea (in Chinese). Chin Sci Bull (Chin Ver), 2002, 47: 235–237
19 Chen J F, Zheng L F, Wiesner M G, et al. Estimate of primary production and export production based on sediment trap in surface layer of South China Sea (in Chinese). Chin Sci Bull (Chin Ver), 1998, 43: 639– 641
20 Dean W E, Gardner J V, Piper D Z. Inorganic geochemical indicators of glacial-interglacial changes in productivity and anoxia on the California continental margin. Geochim Cosmochim Acta, 1997, 61: 4507–4518
21 Algeo T J, Kuwahara K, Sano H, et al. Spatial variation in sediment fluxes, redox conditions, and productivity in the Permian-Triassic Panthalassic Ocean. Palaeogeogr Palaeoclimatol Palaeoecol, 2011, 308: 65–83
22 Qin J, Zhong N N, Qi W, et al. Organic Petrology of the Hongshuizhuang Formation in northern North China (in Chinese). Oil Gas Geol, 2010, 31: 367–374
23 Wang H Z, Qiao X F. Proterozoic stratigraphy and tectonic frame work of China. Geol Mag, 1997, 125: 599–614
24 Liu Y Q. Tectonic cyclic sequences in the mesoproterozoic and Neoproterozoic aulacogen of Yanshan—A concept of aulacogen tectonic cycle and its hierarchy (in Chinese). Acta Geosci Sin, 1997, 18: 142–149
25 Gao L Z, Zhang C H, Shi X Y, et al. A new SHRIMP age of the Xiamaling Formation in the North China Plate and its geological significance. Acta Geol Sin, 2007, 81: 1103–1109
26 Gao L Z, Zhang C H, Shi X Y, et al. Mesoproterozoic age for Xiamaling formation in North China Plate indicated by zircon SHRIMP dating. Chin Sci Bull, 2008, 53: 2665–2671
27 Li H K, Lu S N, Li H M, et al. Zircon and beddeleyite U-Pb precision dating of basic rock sills intruding Xiamaling Formation, North China (in Chinese). Geol Bull Chin, 2009, 28: 1396–1404
28 Su W B, Li H K, Huff W D, et al. SHRIMP U-Pb dating for a K-bentonite bed in the Tieling Formation, North China. Chin Sci Bull, 2010, 55: 3312–3323
29 Wen X D. Lithofacies-palaeogeography and their evolution of the middle-upper Proterozoic in North China (in Chinese). J Univ Petrol Chi, 1989, 13: 13–21
30 Wang J, Chen J F. Study on the environment and potential of source rocks in North China Platform of Middle-Upper Proterzoic (in Chinese). Nat Gas Geosci, 2001, 12: 27–35
31 Duan J Y, Liu P J. Abysmal and sub-abysmal deposit of mesoproterozoic in Yanshan aulocogen, north China (in Chinese). J Jilin Univ, 2003, 33: 7–12
32 Bao Z D, Chen J F, Zhang S C, et al. Study on sedimentary environment and controlled factors of hydrocarbon rock of Mesoproterozoic and Neoproterozoic in North China (in Chinese). Sci China Ser D-Earth Sci, 2004, 34: 114–119
33 Zhabina N N, Volkov I I. A method of determination of various sulfur compounds in sea sediments and rocks. Ann Arbor Sci, 1978, 735–746
34 Canfield D E, Raiswell R, Westrich J T, et al.The use of chromium reduction in the analysis of reduced inorganic sulfur in sediments and shales. Chem Geol, 1986, 54: 149–155
35 Gorjan P, Veevers J J, Walter M R. Neoproterozoic sulfur-isotope variation in Australia and global implications. Precambrian Res, 2000, 100: 151–179
36 Berner R A, Raiswell R. Burial of organic carbon and pyrite sulphur in sediments over Phanerozoic time: A newtheory. Geochim Cosmochim Acta, 1983, 47: 855–862
37 Leventhal J S. An interpretation of carbon and sulfur relationships in Black Sea sediments as indicators of environments of deposition. Geochim Cosmochim Acta, 1983, 47: 133–138
38 Leventhal J S. Carbon and sulfur relationships in Devonian shales from the Appalachian Basin as an indicator of environment of deposition. Amer J Sci, 1987, 287: 33–49
39 Raiswell R, Berner R A. Pyrite formation in euxinic and semi-euxinic sediments. Amer J Sci, 1985, 285: 710–724
40 Sadiq M. Thermodynamic solubility relationships of inorganic vanadium in the marine environment. Mar Chem, 1988, 23: 87–96
41 Van der Sloot H A, Hoede D, Wijkstra J, et al. Anionic species of V, As, Se, Mo, Sb, Te and W in the Scheldt and Rhine estuaries and the Southern Bight (North Sea). Estua Coastal Shelf Sci, 1985, 21: 633–651
42 Wanty R B, Goldhaber R. Thermodynamics and kinetics of reactions involving vanadium in natural systems: Accumulation of vanadium in sedimentary rock. Geochim Cosmochim Acta, 1992, 56: 171–183
43 Breit G N, Wanty R B. Vanadium accumulation in carbonaceous rocks: A review of geochemical controls during deposition and diagenesis. Chem Geol, 1991, 91: 83–97
44 Emerson S R, Huested S S. Ocean anoxia and the concentrations of molybdenum and vanadium in seawater. Mar Chem, 1991, 34: 177–196
45 Morford J L, Emerson S. The geochemistry of redox sensitive trace metals in sediments. Geochim Cosmochim Acta, 1999, 63: 1735–1750
46 Tribovillard N, Algeo T W, Lyons T, et al. Trace metals as paleoredox and paleoproductivity proxies: An update. Chem Geol, 2006, 232: 12–32
47 Cranston R E, Murray J W. The determination of chromium species in natural waters. Anal Chim Acta, 1978, 99: 275–282
48 Elderfield H. Chromium speciation in sea water. Earth Planet Sci Lett, 1970, 9: 10–16
49 Achterberg E P, van den Berg C M G, Boussemart M, et al. Speciation and cycling of trace metals in Esthwaite water: A productive English lake with seasonal deep-water anoxia. Geochim Cosmochim Acta, 1997, 61: 5233–5253
50 Huerta-Diaz M A, Morse J W. Pyritisation of trace metals in anoxic marine sediments. Geochim Cosmochim Acta, 1992, 56: 2681–2702
51 Morse J W, Luther III G W. Chemical influences on trace metal-sulfide interactions in anoxic sediments. Geochim Cosmochim Acta, 1999, 63: 3373–3378
52 Jones B, Manning D A C. Comparison of geochemical indices used for the interpretation of palaeoredox conditions in ancient mudstones. Chem Geol, 1994, 111: 111–129
53 Broecker W S, Peng T H. Tracers in the Sea. New York: Eldigio Press, 1982
54 Calvert S E, Pedersen T F. Geochemistry of recent oxic and anoxic sediments: Implications for the geological record. Mar Geol, 1993, 113: 67–88
55 Crusius J, Calvert S E, Pedersen T F, et al. Rhenium and molybdenum enrichments in sediments as indicators of oxic, suboxic, and sulfidic conditions of deposition. Earth Planet Sci Lett, 1996, 145: 65–78
56 Helz G R, Miller C V, Charnock J M, et al. Mechanism of

molybdenum removal from the sea and its concentration in black shales: EXAFS evidence. Geochim Cosmochim Acta, 1996, 60, 3631–3642
57 Algeo T J, Maynard J B. Trace-element behavior and redox facies in core shales of Upper Pennsylvanian Kansas-type cyclothems. Chem Geol, 2004, 206: 289–318
58 Brumsack H J. The inorganic geochemistry of Cretaceous black shales (DSDP Leg 41) in comparison to modern upwelling sediments from the Gulf of California. Geol Sot Lond Spec Publ, 1986, 21: 447–462
59 Meyer E E, Burgreen B N, Lackey H, et al. Evidence for basin restriction during syn-collisional basin formation in the Silurian Arisaig Group, Nova Scotia. Chem Geol, 2008, 256: 1–11
60 Arthur M A, Dean W E. Organic matter production and preservation, and evolution of anoxia in the Holocene Black Sea. Paleoceangraphy, 1998, 13: 395–411
61 Piper D Z. Seawater as the source of minor elements in black shales, phosphorites, and other sedimentary deposits. Chem Geol, 1994, 115: 95–114
62 Holland H D. The Chemistry of the Atmosphere and the Oceans. New York: Wiley-Interscience, 1978
63 Tyrrell T. The relative influences of nitrogen and phosphorus on oceanic primary production. Nature, 1999, 400: 525–531
64 Redfield A C. The biological control of chemical factors in the environment. Am Sci, 1958, 46: 205–222
65 Brumsack H J, Gieskes J M. Interstitial water trace metal chemistry of laminated sediments from the Gulf of California, Mexico. Mar Chem, 1983, 14: 89–106
66 Brumsack H J, Zuleger E, Gohn E, et al. Stable and radiogenic isotopes in pore waters from Leg 127, Japan Sea. In: Pisciotto K A, Ingle Jr J C, Von Breymann M T, et al., eds. Proc Ocean Drill Project 127/128, 1992, Part 1, 635–650